HHS Public Access

Author manuscript

J Neuroimmunol. Author manuscript; available in PMC 2017 February 15.

Published in final edited form as:

J Neuroimmunol. 2016 February 15; 291: 18–27. doi:10.1016/j.jneuroim.2015.12.004.

Suppression of microglia activation after hypoxia-ischemia results in age-dependent improvements in neurologic injury

Ulas Cikla[a,*], **Vishal Chanana**[a,*], **Douglas B. Kintner**[a], **Lucia Covert**[a], **Taylor Dewall**[a], **Alex Waldman**[a], **Paul Rowley**[a], **Pelin Cengiz**[a,b], and **Peter Ferrazzano**[a,b,#]

[a]Waisman Center, University of Wisconsin, School of Medicine and Public Health, Madison, WI 53705, USA

[b]Department of Pediatrics, University of Wisconsin, School of Medicine and Public Health, Madison, WI 53705, USA

Abstract

We previously found increased microglial proliferation and pro-inflammatory cytokine release in infant mice compared to juvenile mice after hypoxia-ischemia (HI). The aim of the current study was to assess for differences in the effect of microglial suppression on HI-induced brain injury in infant and juvenile mice. HI was induced in neonatal (P9) and juvenile (P30) mice and minocycline or vehicle was administered at 2 hours and 24 hours post-HI. P9 minocycline-treated mice demonstrated early but transient improvements in neurologic injury, while P30 minocycline-treated mice demonstrated sustained improvements in cerebral atrophy and Morris Water Maze performance at 60 days post-HI.

Keywords

microglia; neonatal hypoxia-ischemia; neuroinflammation; cerebral atrophy

[#]**Address correspondence to:** Peter Ferrazzano, M.D., Department of Pediatrics, University of Wisconsin Medical School, T517 Waisman Center, 1500 Highland Ave., Madison, WI, 53705, Tel: (608) 890-0759, Fax: (608) 263-1409, ferrazzano@pediatrics.wisc.edu.

[*]These authors contributed equally to this work

Ulas Cikla: cikla@wisc.edu
Vishal Chanana: chanana@pediatrics.wisc.edu
Douglas B. Kintner: dkintner@pediatrics.wisc.edu
Lucia Covert: lcovert@wisc.edu
Taylor Dewall: tdewall@wisc.edu
Alex Waldman: awaldman@wisc.edu
Paul Rowley: prawley@wisc.edu
Pelin Cengiz: cengiz@pediatrics.wisc.edu

COMPETING INTERESTS:
None

AUTHOR'S CONTRIBUTIONS: UC carried out behavioral studies and participated in imaging studies; VC participated in the behavioral studies, carried out the flow cytometry studies and participated in the imaging studies; DK carried out the IHC studies, performed statistical analysis and helped draft manuscript; LC, TD and AW participated in the IHC studies; PR participated in the imaging studies; PC participated in the design and coordination of the study; PF coordinated the study and drafted the manuscript.

1. Introduction

Neuroinflammation plays an important role in ischemic brain injury, and modulating the microglia-mediated inflammatory response to ischemia has been considered as a potential target for neuroprotective intervention. However, microglia exhibit a complex response to injury, releasing cytotoxic mediators which may worsen injury (Biran et al., 2006, Deng, 2010, Vexler and Yenari, 2009) , and also expressing immunomodulatory and neurotrophic factors which contribute to healing and recovery from injury (Lalancette-Hebert et al., 2007). The exact contribution that each of these microglial responses plays to a specific injury likely varies depending on the mechanism, location, and severity of the injury, and importantly, may also depend on the age at which the injury occurs.

Microglia are derived from monocytes which originate in the yolk sac and populate the brain during early fetal brain development. In the fetal brain, these immature microglia are ameboid cells likely responsible for phagocytosis of cellular debris which results from brain development and synaptogenesis(Graeber and Streit, 2010). Perinatally, these microglia migrate throughout the brain and transition to a highly ramified immunosurveillance phenotype which is maintained throughout life. This process is thought to occur over the first 2-3 weeks of life in rodents and is complete by post-natal day 30. A growing body of literature has revealed differences in gene expression between neonatal and adult microglia (Butovsky et al., 2014, Parakalan et al., 2012). However, differences in how neonatal and mature microglia respond to injury remain poorly defined.

We previously described that microglia in the neonatal brain respond to hypoxia-ischemia (HI) with increased activation, proliferation, and release of pro-inflammatory mediators compared to juveniles (Ferrazzano et al., 2013a). How the microglial response aggravates or ameliorates injury after hypoxia-ischemia in the developing brain has remained poorly understood. In order to understand age-dependent differences in microglial responses to ischemic brain injury, we determined the effect of microglial inhibition with minocycline on hypoxic-ischemic brain injury in neonatal (P9) and juvenile (P30) mice. Based on our previous findings of a more pro-inflammatory microglial response in neonatal brains, we hypothesized that suppression of microglial activation after HI would result in improved neuronal injury, less cerebral atrophy, and improved memory and learning in P9 mice compared to P30 mice.

2. Methods

2.1 Materials

Mouse monoclonal anti-microtubule associated protein 2 (MAP2) antibody was from Sigma (St. Louis, MO). Iba1 rabbit polyclonal antibody was from Wako Chemical (Richmond, VA). Rat anti-mouse CD45-FITC antibody was from AbD Serotec (Raleigh, NC). Mouse CD11b-APC conjugated antibody, goat anti-mouse Alexa Fluor 488-conjugated IgG and goat anti-rabbit Alexa Fluor 546-conjugated IgG were from Invitrogen (Carlsbad, CA). Vectashield mounting medium with DAPI was from Vector Labs (Burlingame, CA). Tissue-Tek O.C.T. compound was from Sakura Finetek (Torrance, CA). Hanks balanced salt solution (HBSS) was obtained from Mediatech Cellgro (Manassas, VA).

2.2 Animal usage

All procedures on animals were carried out in adherence with NIH Guide for the Care and use of Laboratory Animals and approved by the Institutional Animal Care and Use Committee at the University of Wisconsin-Madison.

2.3 Induction of hypoxia-ischemia

Using the Vannucci model of neonatal hypoxia-ischemia (Gurd et al., 1999), HI was induced in P9 and P30 mice as described previously (Ferrazzano et al., 2013b). C57BL/6J mice (P9 and P30) were anesthetized with isoflurane (3% for induction, 1.5% for maintenance), in 30% O_2 and 70% N_2O. The duration of anesthesia was kept to less than 5 min in each animal to minimize any potential effects of isoflurane on neuronal injury or microglial activation (Wu et al., 2012, Xie et al., 2008, Zhang et al., 2012). The body temperature of the animal was maintained at 37°C with a heated surgical platform (Patterson Scientific, Bend, OR). Under a Nikon SMZ-800 stereo surgical microscope (Nikon Instruments, Mellville, NY), a midline skin incision was made and the left common carotid artery was dissected out and electrically cauterized as described previously (Cengiz et al., 2011). The incision was superfused with 0.5% bupivacaine and closed with a 6.0 silk suture. Animals were returned to their dams and monitored continuously for the initial 30 min during a 2 h recovery period. The animals were then placed in a hypoxia chamber (BioSpherix Ltd, Redfield, NY) equilibrated with 10% O_2 and 90% N_2 at 37°C for 50 min. In this model, the unilateral carotid artery cauterization by itself induces no injury because perfusion is maintained through collateral circulation. However, on subsequent exposure to hypoxia a unilateral ischemia occurs as blood flow decreases to the hemisphere ipsilateral to the cauterized carotid artery (Mujsce et al., 1990). After HI, animals were monitored continuously for the initial 30 min of reoxygenation and then checked every 30 min for 2 h and then daily until sacrificed. At 2 h and 24 h post-HI animals were given either minocycline (40 mg/kg, i.p. total volume = 0.2 ml) or vehicle (sterile saline).

2.4 Flow cytometry analysis of brain microglia cells

At day 2 or 9 after HI, mice were deeply anesthetized with 5% isoflurane plus N_2O and O_2 (3: 2) and decapitated. Immediately after decapitation, cerebellums and meninges were removed. The contralateral and ipsilateral hemispheres were separated, and the hippocampus, cortex and striatum were dissected from each hemisphere and submerged into ice-cold Hank's balanced salt solution (HBSS). Samples of each brain region were pooled from 5 mice for analysis. Brain tissues were cut into small pieces and dissociated into a single cell suspension by gentle physical disruption and enzymatic digestion using a commercially available tissue dissociation kit according to manufacturer's instructions (Miltenyi Biotech Inc. Auburn, CA). Myelin was removed by centrifugation of the sample in 0.9M sucrose in HBSS at 2200 g for 10 min at 4°C and cells were rinsed in HBSS and collected after passing through a 40 μm membrane by centrifugation.

For flow cytometry analysis, the cell suspension was first incubated with 10% goat serum in 0.1M PBS (pH 7.4) for 20 min at room temperature. After the incubation, cells were centrifuged at 200 g for 5 min. The supernatant was then aspirated and the pellet was suspended (~ 10^6 cells/ml) in 4% paraformaldehyde (PFA) in 0.1 M PBS and incubated for

30 min at room temperature on an orbital shaker. Cells were then centrifuged at 1000 g for 5 min and washed with 0.1M PBS to remove excess fixation buffer. The fixed cells (~10^6 cells) in 0.1 ml PBS were incubated with APC-conjugated rat anti-mouse CD11b and FITC-conjugated rat anti-mouse CD45 antibodies (25 μL of 0.2 mg/ml) for 30 min in ice. Cells were rinsed with 0.1M PBS by centrifugation for 5 min at 1000 g and pellets were suspended in 500 μl of 0.1M PBS and acquired immediately with a FACSCalibur flow cytometer running CellQuest Pro software (BD Biosciences, San Jose, CA) with the following settings: Forward scatter V = E00, gain = 1.0, mode = Lin; Side scatter V = 399, gain = 1.25, mode = Lin; FL1 V = 572, gain = 1.0, mode = Log; FL4 V = 704, mode = Log. In each experiment, 10,000 events were acquired for analysis from each sample. $CD11b^+$/$CD45^+$ cells were quantified in each brain region and expressed as the ratio of ipsilateral to contralateral cell counts.

2.5 Immunofluorescence staining

Mice were deeply anesthetized with 5% isoflurane plus N_2O and O_2 (3: 2) and transcardially perfused with 4% PFA in 0.1 M PBS. Brains were post-fixed in 4% PFA in 0.1 M PBS for 12 h, and subsequently cryoprotected with 30% sucrose in 0.1 M PBS for 24-36 h at 4°C. The brains were frozen in an optimal cutting temperature compound for 10 min and cut into 35 μm coronal sections on a freezing microtome (Leica SM 2000R; Buffalo Grove, IL), and stored in antifreeze solution at −20°C.

2.5.1 Neurological Scoring—Sections at the level of 0.02 mm anterior from bregma (anterior), 1.70 mm posterior from bregma (hippocampal), and 2.70 mm posterior from the bregma (posterior) were selected from each brain and processed for neurological scoring. Sections were rinsed 3 X 10 min in 0.1 M Tris-buffered saline (TBS, pH 7.4), and incubated with a blocking solution (0.1% Triton X-100 and 3% goat serum in 0.1 M TBS) for 30 min at 37 °C. Sections were incubated with mouse anti-MAP2 (1:500) in blocking solution for 1 h at 37 °C and then overnight at 4°C. After rinsing 3 X 10 min in 0.1 M TBS, sections were incubated with goat anti-mouse Alexa Fluor 488-conjugated IgG in blocking solution (1:200) for 1 h at 37 °C. Sections were rinsed 3 X 10 min in 0.1 M TBS and then mounted on slides with vectashield mounting media. For neurological scoring, stitched whole brain fluorescent images (FITC) were captured on a Zeiss upright epifluorescent photomicroscope equipped with a motorized stage, 2.5X lens and a CDD camera driven by Stereo Investigator software (MBF Bioscience, Williston, VT). A blinded investigator scored the whole brain images using a scoring system modified from Sheldon et al. (Sheldon et al., 1998). Briefly, ipsilateral and contralateral brain regions were compared (anterior cortex, dentate gyrus, CA1, CA2, CA3, hippocampal cortex, hippocampal striatum, posterior cortex) and each region assigned a score of 0-3 (0 = no loss of MAP2 staining, normal dendritic morphology; 1= some loss of MAP2 staining, disturbed dendritic morphology, hippocampal shrinkage, ventriculomegaly and cortical thinning; 2= moderate loss of MAP2 staining, disturbed dendritic morphology, hippocampal shrinkage, ventriculomegaly and cortical thinning; 3 = total loss of MAP2 staining, gross infarction and loss of structures within the region). The score for the eight regions were summed to give a total injury score ranging from 0 (no damage) to 24 (severe damage). Animals that died during the reoxygenation period were assigned the maximum injury score of 24.

2.5.2 Microglial morphology—To demonstrate microglial morphology, sections at the level of hippocampus (1.70 mm posterior from bregma) from each brain were double stained as above using rabbit anti-Iba1 (1:250) and mouse anti-MAP2 (1:500) as primary antibodies and goat anti-rabbit Alexa Fluor 488-conjugated IgG and goat anti-mouse Alexa Fluor 546-conjugated IgG as secondary antibodies. Sections were then mounted on slides with vectashield with DAPI mounting medium. For negative controls, brain sections were stained with the secondary antibody only. Sections stained for Iba1/MAP2 was sequentially imaged on a Nikon A1 confocal microscope for DAPI (blue), Iba1 (green) and MAP2 (red). Contralateral and ipsilateral images of the CA1, cortex and striatum regions were acquired using 20X, and 60X objectives. In addition, digital zoom was used to acquire a 240X image of each region. Identical acquisition settings were used to capture all images.

2.6 Magnetic Resonance Imaging (MRI)

MRI was performed using a Varian 4.7T Small Animal MRI scanner. Mice were anesthetized with 1.5% isoflurane in an oxygen/air mixture administered through a nose cone and then secured in a cradle positioned within the center of the magnet bore. Respiratory rate and body temperature were monitored with a MR-compatible physiology monitoring unit, and temperature was maintained within physiologic limits using a heated airflow unit. T2-weighted fast spin-echo images (TR = 4000 ms, effective TE = 60 ms, echo train length = 8, matrix size 128 × 128, averages = 40) were acquired in twelve contiguous axial slices with a field of view of 17 × 17 mm and a slice thickness of 1 mm. Masks of intact tissue (excluding ventricles and cysts) in ipsilateral and contralateral hemispheres were manually traced for each slice by a blinded investigator using the FMRIB Software Library (FSL, Oxford, UK) image analysis program. Hemispheric tissue volumes were calculated and expressed as a ratio of ipsilateral/contralateral tissue volumes.

2.7 Morris Water Maze (MWM)

Spatial learning was assessed by the MWM test at P60 (51 days post-HI) on HI-vehicle control and minocycline-treated mice as described previously (Uluc et al., 2013). Mice were trained to locate a hidden escape platform in a circular pool full of opaque water by use of visual cues. The pool was equipped with the clear acrylic hidden escape platform and a Panasonic Digital CCTV (Model WV-BP334) camera and a Piccolo Diligent video capture board plus Noldus Instruments EthoVison XT software (Leesburg, VA). The pool was virtually divided into equal quadrants with four virtual points, west, north, east, and south. The escape platform was placed in the center of the NW quadrant (Q1).

Mice were transported from the housing room to the testing room, and were allowed to acclimate to the room for 30 min before training or testing. Testing was performed by a researcher blinded to treatment group. A brief preliminary training was conducted with each mouse to ensure it could swim and climb onto the platform. Each mouse was trained for 4 trials per block, 2 blocks /day for 4 days (a total of 32 trials). Between each trial, mice were allowed to rest on the platform for 10-15 sec. Trials lasted 1 min, or until the mouse found the platform. If the mouse did not find the platform, it was placed on the platform for 10-15 sec by the researcher. The time to reach the platform was automatically tracked and recorded. After trial 32, each animal was given a probe trial, during which the platform was

removed from Q1 and each animal was allowed 60 sec to search for the platform in the pool. The number of times the animal swam over the platform location in the training quadrant (Q1) and the corresponding area in quadrants 2-4 was recorded and reported as platform crossings.

2.8 Statistical analysis

Values are expressed as the mean ± SEM. Statistical analysis was performed using SigmaPlot (Systat Software, San Jose, CA). To determine group differences in microglia counts and hemispheric volumes, two way ANOVA was used with Bonferroni post-test to correct for multiple comparisons. For analysis of injury scoring, the Kruskal-Wallace non-parametric test for analysis of variance was used with Dunn's post-test. For analysis of time-to-platform in MWM testing, repeated measures ANOVA was performed. P-values smaller than or equal to 0.05 were considered statistically significant.

3. Results

3.1 Minocycline suppresses HI-induced microglia counts in P9 and P30 brains

In this study, minocycline or vehicle was administered at 2 hours and 24 hours post-HI, and the effect of minocycline on microglial responses was determined using flow cytometry and immunostaining. The effect of microglial suppression after HI on acute and chronic neurologic outcome was assessed using immunostaining, MRI and behavioral testing.

To assess the effect of minocycline on microglial responses post-HI, we used flow cytometry to quantify the number of $CD11b^{+}/CD45^{+}$ cells in ipsilateral and contralateral hippocampus, cortex and striatum in P9 and P30 mice with and without minocycline treatment. Ipsilateral microglia counts were normalized to the counts in the corresponding contralateral hemisphere (IL/CL), (**Figure 1**). At 2 days post-HI, HI induced a robust increase in microglia counts in the ipsilateral hippocampus of non-treated P9 mice (~ 9.5 fold), and less microglia proliferation in P30 hippocampus (~5.7 fold) (**Figure 1 A**), similar to what we reported previously(Ferrazzano, Chanana, 2013a). By comparison, in cortex and striatum the increase in ipsilateral microglial population in P9 and P30 at day 2 post-HI was comparatively modest (1.7 - 3.5 times) (**Figure 1 B, C**). Minocycline treatment resulted in a significant reduction in microglia counts in the ipsilateral hippocampus in both P9 and P30 brains at 2 days post-HI (**Figure 1 A**).

By 9 days post-HI, the ipsilateral cortex and striatum in non-treated P9 and P30 mice demonstrated a dramatic increase in microglia counts (~5.2 – 8.8 fold). Interestingly, ipsilateral microglia counts remained significantly suppressed in minocycline-treated P9 mice at 9 days post-HI, while the P30 cortex and striatum demonstrated a rebound increase in ipsilateral microglia counts despite early minocycline therapy (**Figure 1 B, C**).

3.2 Minocycline suppresses microglia activation in P9 and P30 mice

To further assess the microglial response post-HI, we next analyzed the $CD11b^{+}/CD45^{+}$ population of cells based on differential CD45 expression levels. As previously described, CD45 expression can be used to characterize the activation state of microglia (Campanella et

al., 2002, Denker et al., 2007, Ferrazzano, Chanana, 2013a, Stevens et al., 2002), where low signal is associated with quiescent microglia, medium intensity with activated microglia and high signal labeling blood-born monocytes. In the current study, less than 1% of the $CD11b^{+}/CD45^{+}$ population demonstrated $CD45^{high}$ expression, similar to our prior studies(Ferrazzano, Chanana, 2013a). **Figure 2 A-C,** shows the percentage of $CD45^{medium}$ activated microglia in P9 and P30 brains at day 2 and day 9 post-HI in hippocampus, cortex and striatum. In contralateral brain regions, $CD45^{med}$ cells represented a small fraction (~2-7%) of the overall microglia population in both P9 and P30 mice regardless of minocycline treatment, and no $CD45^{high}$ cells were detected. At day 2 post-HI in untreated P9 and P30 ipsilateral hippocampi, the percentage of $CD45^{medium}$ microglia increased to ~ 33% (**Figure 2 A**). Minocycline treatment resulted in a significant reduction (~70%) in the proportion of the $CD11b^{+}/CD45^{+}$ population demonstrating $CD45^{medium}$ expression at day 2 in both P9 and P30 ipsilateral hippocampus.

Similar to the quantification of microglia counts post-HI, the microglial activation in the cortex and striatum in untreated mice increased at 9 days post-HI. Minocycline-treated P9 mice demonstrated a significant decrease in the percentage of activated microglia in ipsilateral cortex and striatum at day 9 post-HI (**Figure 2 B, C**), while this late microglia activation was not suppressed minocycline in the P30 mice.

3.3 Changes in microglial morphology post-HI are inhibited by minocycline

To visualize the changes in microglial morphology, brain slices were stained for Iba-1 (microglia), MAP2 (neuronal dendrites) and DAPI (nucleus) and images collected in the hippocampus (**Figure 3**), cortex (**Figure 4**) and striatum (**Figure 5**). Time-points shown reflect the peak microglial activation detected by flow cytometry in each brain region. In the CA1 region of the contralateral hippocampus at 2 days post-HI, microglia are largely distributed outside the cell body layer (**Figure 3 a, c, e, and g)** and demonstrated a ramified morphology with small somas and extensive arborization of cell processes typical of surveillance-state microglia (**Figure 3; Insets: a, c, e, and g).** At day 2 post-HI in the untreated neonatal and juvenile ipsilateral hippocampi, microglia had migrated to the cell body layer of CA1 (**Figure 3 b, d**) and transformed into an activated phenotype with decreased cell processes or an amoeboid morphology (**Figure 3; Insets: b and d**). With minocycline treatment, the microglia in the ipsilateral hippocampus are distributed outside the cell body layer (**Figure 3 f and h**) and retained a ramified morphology indicating decreased microglial activation in these brains (**Figure 3; Insets f and h**) similar to the contralateral hemispheres.

In the contralateral cortex and striatum, microglia are evenly distributed (**Figures 4 & 5; Insets a, c, e, and g)** and demonstrated a ramified morphology (**Figure 4; Insets a, d, e, and g).** In both P9 and P30 non-treated ipsilateral cortex and striatum, microglia demonstrate an activated morphology (**Figures 4 & 5; Insets b, d).** In minocycline-treated P9 mice, microglia demonstrate a ramified morphology in the cortex and striatum at day 9 post-HI (**Figure 4 & 5; Inset f**). However, at day 9 in minocycline-treated P30 mice, microglia in ipsilateral cortex and striatum display activated morphology similar to that seen in the vehicle-treated controls (**Figure 4 & 5; Inset h**).

3.4 Minocycline improves acute neurologic injury after HI in neonatal mice

Next, we determined whether differential microglial activation in P9 and P30 brains is related to the degree of neurologic damage in the first 9 days post-HI. HI resulted in loss of MAP2 staining and tissue loss primarily in the hippocampus in both neonatal and juvenile brains (**Figure 6 A, arrow**). Summary of neurological damage scores are presented in **Figure 6 B**. HI resulted in moderate injury in non-treated P9 control mice at day 2 (14.2±2.0) and day 9 (15.8±2.8) post-HI. Minocycline-treated P9 mice demonstrated a significant reduction in neurologic injury score at day 2 (73% reduction) and day 9 (87% reduction) post HI. HI induced a somewhat less severe injury in the P30 mice at day 2 (8.6±3.3) and day 9 (9.6±3.5) post-HI, and no significant improvement in injury score was seen in minocycline-treated P30 mice at either time-point.

3.5 Minocycline improves HI induced cerebral atrophy in juvenile but not neonatal mice

In order to determine whether minocycline resulted in a sustained effect on neurological injury, T2-weighted MRI was performed at 9 days and 60 days post-HI, and ipsilateral hemispheric volume loss was calculated (**Figure 7**). At day-9 post-HI, mild ipsilateral ventriculomegaly and tissue volume loss was seen in some non-treated P9 mice which did not reach statistical significance (**Figure 7 A, B**). As the HI model does not induce gross infarction, we did not anticipate identifying significant injury at this early time-point using T2-weighted MRI. In contrast, at 60 days post-HI, T2-weighted images in non-treated P9 mice revealed moderate ventriculomegaly and cortical thinning resulting in ~15% volume loss in the ipsilateral hemisphere relative to the uninjured contralateral hemisphere (**Figure 7 C**). Minocycline-treated P9 mice demonstrated significant ipsilateral hemispheric volume loss similar to the non-treated animals. HI induced a moderate but significant ipsilateral hemispheric volume loss in vehicle-treated P30 mice (~8%). Hemispheric volume was preserved in minocycline-treated P30 mice similar to that seen in the sham operated animals. Therefore, minocycline treatment resulted in less cerebral atrophy in P30 but not P9 mice at 60 days post-HI.

3.6 Minocycline treatment restores hippocampal learning in P30 but not P9 mice at 60 days post-HI

In order to determine whether minocycline treatment resulted in sustained improvements in memory and learning, MWM testing was performed in P9 and P30 mice at 60 days post-HI. The MWM test is designed to detect deficits in cognitive performance in a spatially oriented task and is correlated to the degree of hippocampal injury (McAuliffe et al., 2006). As seen in **Figure 8**, in both P9 and P30 sham groups, the time for the mouse to find the platform decreased over the four days of training (**Figure 8 A, B**), indicating learning of the task Vehicle-treated P9 and P30 mice exposed to HI did not improve the time-to-platform over the course of the training period, indicating impaired learning. Minocycline-treated P30 mice demonstrated significant improvement in time-to-platform over the training period similar to the sham operated mice, while minocycline treated P9 mice failed to learn the task. During the probe trial (**Figure 8 C, D**), sham operated P9 and P30 mice demonstrated significantly more platform crossings in the training quadrant, indicating spatially oriented learning and memory in these animals. Exposure to HI induces impairments in spatial

learning and memory in both P9 and P30 mice as evidenced by the lack of quadrant-based discrimination in platform crossings. Minocycline-treated P30 mice demonstrated significantly more platform crossings in the training quadrant, indicating improved spatial memory and learning in this group (**Figure 8 D**), while no improvement in the platform-crossing measure was seen in minocycline-treated P9 mice.

4. Discussion

4.1 The role of microglia in the developing brain

Microglia are derived from myeloid precursor cells which invade the brain during early embryonic development (Czeh et al., 2011). Immature microglia are amoeboid, phagocytic cells that play a role in clearance of the cellular debris which occurs during brain development (Czeh, Gressens, 2011, Paolicelli et al., 2011). During late fetal development, microglia begin to transition from activated phagocytic cells into an immunosurveillance cell with a highly ramified morphology, a process which continues post-natally in humans and rodents (Hristova et al., 2010, Vexler and Yenari, 2009).

The effect of microglial maturation state on the subsequent microglial response to an injury is poorly understood. We previously demonstrated that microglia in the P9 brain respond to HI with greater proliferation and pro-inflammatory cytokine release compared to P30 brains (Ferrazzano, Chanana, 2013a). In the current study, we similarly found that P9 mice demonstrated a greater increase in microglia counts compared to P30 mice in the hippocampus early after injury. It is increasingly recognized that microglia have diverse functions in both the developing and mature brain. Microglia play a role in synaptic pruning, neuronal differentiation, and astrocytic proliferation (Czeh, Gressens, 2011, Marin-Teva et al., 2004, Paolicelli, Bolasco, 2011, Walton et al., 2006), and their function varies by region (de Haas et al., 2008, Hristova, Cuthill, 2010). In the current study, we found a biphasic microglial response in P9 and P30 mice after HI, with an early increase in microglia counts and microglial activation in the hippocampus, and a later increase in the cortex and striatum, similar to what we found previously(Ferrazzano, Chanana, 2013a). The implications of this biphasic regional microglia response on injury and recovery have remained unclear, and prompted our investigation into the effect of microglial inhibition after HI.

4.2 Effect of Minocycline on microglia responses and brain injury

To study the effect of inhibiting microglial responses after HI, we first established that administration of minocycline at 2 hours and 24 hours post-HI effectively suppressed the expected HI-induced microglial proliferation and activation in the hippocampus at day 2 post-HI in both P9 and P30 mice. Interestingly, we also found that the expected late increase in microglia counts in the cortex and striatum was suppressed in P9 minocycline-treated mice. This was not the case in the P30 minocycline-treated mice which demonstrated the expected late increase in microglia counts and activation in the cortex and. The half-life of minocycline is approximately 3 hours in rodents (Fagan et al., 2004), therefore continued inhibition of microglia activation by minocycline is unlikely to account for the persistently suppressed microglia counts seen in the P9 minocycline-treated mice. At day-2 and day-9 post-HI, minocycline-treated P9 mice demonstrated a dramatic reduction in neuronal injury.

This early improvement in injury may in turn explain the persistent lack of microglial activation in these mice. The association between early microglial inhibition and improved neuronal injury supports a cytotoxic role for the early microglial response in P9 mice. Our findings are consistent with a number of studies which have demonstrated early improvements in neurologic injury with minocycline treatment after hypoxia-ischemia in the neonatal brain (Buller et al., 2009). For example, Fan et al. found that pretreatment with minocycline in a P4 rat model of HI resulted in decreased neurologic injury and improved neurologic function when assessed at P21 (Fan et al., 2006). Similarly, Carty et al. reported decreased injury on day 7 post-HI in a P3 rat model, when minocycline was administered at 2 hours post-HI and continued daily for 7 days (Carty et al., 2008).

Given the dramatic improvement seen early after injury in minocycline-treated P9 mice in our study, the results from our assessments of cerebral atrophy and behavioral outcome at 60 days post-HI were surprising. MRI at 60 days post-HI revealed significant atrophy in P9 minocycline-treated mice similar to non-treated controls, and MWM testing revealed impaired memory and learning in these minocycline-treated mice as well. Early improvement in injury from minocycline treatment but no lasting improvement in cerebral atrophy or behavioral outcome has been observed previously in other models of developmental brain injury. For example, Fox et al. found that early improvements in infarct size in minocycline-treated neonatal rats exposed to transient middle cerebral artery occlusion were not sustained out to 1 week post-injury (Fox et al., 2005). Minocycline has not been reported to improve long-term cerebral atrophy or neurologic function at chronic time-points after neonatal HI.

Our finding that minocycline treatment improves cerebral atrophy and learning in juvenile but not neonatal mice is novel. In contrast to the P9 mice in our study, the P30 minocycline-treated mice demonstrated significant improvement in hemispheric volume loss and improvements in memory and learning at 60 days post-HI. The mechanism underlying this discrepancy in the effect of minocycline treatment between the neonatal and juvenile brain remains unknown. However, the lack of a delayed increase in microglia activation in the P9 minocycline-treated mice at day 9 post-HI may contribute to this injury profile. A number of studies have described a transition in the microglial response during recovery from an injury, with an early pro-inflammatory and cytotoxic microglial response (M1) followed by a subsequent immunomodulatory and neurotrophic response (M2) (Bonestroo et al., 2013, Shrivastava et al., 2013, Soehnlein and Lindbom, 2010, Varin and Gordon, 2009). Our results suggest that the delayed microglial response may be critical to improvements in cerebral atrophy, as the juvenile minocycline-treated mice in our study mounted this late microglial response and subsequently demonstrated long-term improvements in atrophy and neurologic function. To confirm the role of the late microglial response to injury in the developing brain, further studies will be needed to define the time-course of M1 and M2 responses after HI, and to assess the effect of a prolonged course of microglial inhibition on long-term neurologic injury.

Minocycline has pleiotropic effects which must be considered when interpreting our results. In addition to the well-described suppression of microgliosis, minocycline also has been shown to inhibit matrix metalloproteinases (Machado et al., 2006, Nagel et al., 2008) and

exhibits anti-apoptotic (Wang et al., 2004) and anti-oxidant (Morimoto et al., 2005) properties. While minocycline treatment clearly resulted in suppression of microglial responses after HI in our study, we cannot exclude the possibility of direct effects of minocycline on neuronal survival. However, minocycline has been widely used as an inhibitor of microglia in studies of microglia function. Additionally, it is a clinically relevant pharmacologic agent, it is safe for use in humans and it has been investigated in early stage clinical trials for treatment of neurologic injuries such as stroke (Kohler et al., 2013) and spinal cord injury (Casha et al., 2012).

Our findings have implications for the therapeutic potential of microglial suppression after HI, as the impact of microglial inhibition on outcome after injury is age-dependent. While minocycline therapy improved long-term injury in juvenile mice, in neonatal mice it results in only transient improvement in neurologic injury after HI. Importantly, our findings demonstrate that early improvements in neurologic injury do not necessarily predict long-term improvements in neurologic function. Furthermore, neonatal brains may benefit from therapies aimed at enhancing or augmenting the late neurotrophic microglial response..

5. Conclusions

In this study, we found that microglial inhibition with minocycline had differential effects on neurologic outcome after HI depending on the age at which the injury was induced. In P9 mice, minocycline treatment after HI improved early neurologic injury, but did not result in sustained improvements in cerebral atrophy or memory impairments. In P30 mice, minocycline treatment resulted in decreased cerebral atrophy and improved memory and learning at 2 months post-HI. These age-dependent differences in the effect of minocycline have implications on the therapeutic potential of microglial inhibitors after HI injury in the developing brain. Further studies are needed to better understand how the role of microglia in HI-induced neurologic injury differs with age.

ACKNOWLEDGEMENTS

Funding support from: KL2 TR000428 (Cengiz P), NIH P30 HD03352 (Waisman Center), NIH/NINDS 1K08NS078113 (Ferrazzano P).

Abbreviations

HI	Hypoxia ischemia
MAP2	microtubule associated protein 2
HBSS	Hank’s balanced salt solution
PFA	paraformaldehyde
MWM	Morris Water Maze
IL	ipsilateral
CL	contralateral
MRI	Magnetic Resonance Imaging

REFERENCES

Biran V, Joly LM, Heron A, Vernet A, Vega C, Mariani J, Renolleau S, Charriaut-Marlangue C. Glial activation in white matter following ischemia in the neonatal P7 rat brain. Exp. Neurol. 2006; 199:103–12. [PubMed: 16697370]

Bonestroo HJ, Nijboer CH, van Velthoven CT, Kavelaars A, Hack CE, van Bel F, Heijnen CJ. Cerebral and hepatic inflammatory response after neonatal hypoxia-ischemia in newborn rats. Dev. Neurosci. 2013; 35:197–211. [PubMed: 23689428]

Buller KM, Carty ML, Reinebrant HE, Wixey JA. Minocycline: a neuroprotective agent for hypoxic-ischemic brain injury in the neonate? J. Neurosci. Res. 2009; 87:599–608.

Butovsky O, Jedrychowski MP, Moore CS, Cialic R, Lanser AJ, Gabriely G, Koeglsperger T, Dake B, Wu PM, Doykan CE, Fanek Z, Liu L, Chen Z, Rothstein JD, Ransohoff RM, Gygi SP, Antel JP, Weiner HL. Identification of a unique TGF-beta-dependent molecular and functional signature in microglia. Nat Neurosci. 2014; 17:131–43. [PubMed: 24316888]

Campanella M, Sciorati C, Tarozzo G, Beltramo M. Flow cytometric analysis of inflammatory cells in ischemic rat brain. Stroke. 2002; 33:586–92. [PubMed: 11823674]

Carty ML, Wixey JA, Colditz PB, Buller KM. Post-insult minocycline treatment attenuates hypoxia-ischemia-induced neuroinflammation and white matter injury in the neonatal rat: a comparison of two different dose regimens. Int. J. Dev. Neurosci. 2008; 26:477–85. [PubMed: 18387771]

Casha S, Zygun D, McGowan MD, Bains I, Yong VW, Hurlbert RJ. Results of a phase II placebo-controlled randomized trial of minocycline in acute spinal cord injury. Brain. 2012; 135:1224–36. [PubMed: 22505632]

Cengiz P, Kleman N, Uluc K, Kendigelen P, Hagemann T, Akture E, Messing A, Ferrazzano P, Sun D. Inhibition of Na+/H+ exchanger isoform 1 is neuroprotective in neonatal hypoxic ischemic brain injury. Antioxid. Redox Signal. 2011; 14:1803–13. [PubMed: 20712402]

Christensen LB, Woods TA, Carmody AB, Caughey B, Peterson KE. Age-related differences in neuroinflammatory responses associated with a distinct profile of regulatory markers on neonatal microglia. J. Neuroinflammation. 2014; 11:70. [PubMed: 24708744]

Czeh M, Gressens P, Kaindl AM. The yin and yang of microglia. Dev. Neurosci. 2011; 33:199–209. [PubMed: 21757877]

de Haas AH, Boddeke HW, Biber K. Region-specific expression of immunoregulatory proteins on microglia in the healthy CNS. Glia. 2008; 56:888–94. [PubMed: 18338796]

Deng W. Neurobiology of injury to the developing brain. Nat. Rev. Neurol. 2010; 6:328–36. [PubMed: 20479779]

Denker SP, Ji S, Dingman A, Lee SY, Derugin N, Wendland MF, Vexler ZS. Macrophages are comprised of resident brain microglia not infiltrating peripheral monocytes acutely after neonatal stroke. J. Neurochem. 2007; 100:893–904. [PubMed: 17212701]

Fagan SC, Edwards DJ, Borlongan CV, Xu L, Arora A, Feuerstein G, Hess DC. Optimal delivery of minocycline to the brain: implication for human studies of acute neuroprotection. Exp. Neurol. 2004; 186:248–51. [PubMed: 15026261]

Fan LW, Lin S, Pang Y, Rhodes PG, Cai Z. Minocycline attenuates hypoxia-ischemia-induced neurological dysfunction and brain injury in the juvenile rat. Eur. J. Neurosci. 2006; 24:341–50. [PubMed: 16836639]

Ferrazzano P, Chanana V, Kutluay U, Fidan E, Akture E, Kintner DB, Cengiz P, Sun D. Age-dependent microglial activation in immature brains after hypoxia-ischemia. CNS Neurol Disord-DR. 2013a; 12:338–49.

Ferrazzano P, Chanana V, Uluc K, Fidan E, Akture E, Kintner DB, Cengiz P, Sun D. Age-dependent microglial activation in immature brains after hypoxia-ischemia. CNS Neurol. Disord. Drug Targets. 2013b; 12:338–49. [PubMed: 23469850]

Fox C, Dingman A, Derugin N, Wendland MF, Manabat C, Ji S, Ferriero DM, Vexler ZS. Minocycline confers early but transient protection in the immature brain following focal cerebral ischemia-reperfusion. J. Cereb. Blood Flow Metab. 2005; 25:1138–49. [PubMed: 15874975]

Furukawa S, Sameshima H, Yang L, Harishkumar M, Ikenoue T. Regional differences of microglial accumulation within 72 hours of hypoxia-ischemia and the effect of acetylcholine receptor agonist

on brain damage and microglial activation in newborn rats. Brain Res. 2014; 1562:52–8. [PubMed: 24680905]

Graeber MB, Streit WJ. Microglia: biology and pathology. Acta neuropathologica. 2010; 119:89–105. [PubMed: 20012873]

Gurd JW, Bissoon N, Nguyen TH, Lombroso PJ, Rider CC, Beesley PW, Vannucci SJ. Hypoxia-ischemia in perinatal rat brain induces the formation of a low molecular weight isoform of striatal enriched tyrosine phosphatase (STEP). J. Neurochem. 1999; 73:1990–4. [PubMed: 10537057]

Hristova M, Cuthill D, Zbarsky V, Acosta-Saltos A, Wallace A, Blight K, Buckley SM, Peebles D, Heuer H, Waddington SN, Raivich G. Activation and deactivation of periventricular white matter phagocytes during postnatal mouse development. Glia. 2010; 58:11–28. [PubMed: 19544386]

Kohler E, Prentice DA, Bates TR, Hankey GJ, Claxton A, van Heerden J, Blacker D. Intravenous minocycline in acute stroke: a randomized, controlled pilot study and meta-analysis. Stroke. 2013; 44:2493–9. [PubMed: 23868273]

Lalancette-Hebert M, Gowing G, Simard A, Weng YC, Kriz J. Selective ablation of proliferating microglial cells exacerbates ischemic injury in the brain. J. Neurosci. 2007; 27:2596–605. [PubMed: 17344397]

Machado LS, Kozak A, Ergul A, Hess DC, Borlongan CV, Fagan SC. Delayed minocycline inhibits ischemia-activated matrix metalloproteinases 2 and 9 after experimental stroke. BMC Neurosci. 2006; 7:56. [PubMed: 16846501]

Marin-Teva JL, Dusart I, Colin C, Gervais A, van Rooijen N, Mallat M. Microglia promote the death of developing Purkinje cells. Neuron. 2004; 41:535–47. [PubMed: 14980203]

McAuliffe JJ, Miles L, Vorhees CV. Adult neurological function following neonatal hypoxia-ischemia in a mouse model of the term neonate: water maze performance is dependent on separable cognitive and motor components. Brain Res. 2006; 1118:208–21. Epub 2006 Sep 25. [PubMed: 16997287]

Morimoto N, Shimazawa M, Yamashima T, Nagai H, Hara H. Minocycline inhibits oxidative stress and decreases in vitro and in vivo ischemic neuronal damage. Brain Res. 2005; 1044:8–15. [PubMed: 15862784]

Mujsce DJ, Christensen MA, Vannucci RC. Cerebral blood flow and edema in perinatal hypoxic-ischemic brain damage. Pediatr. Res. 1990; 27:450–3. [PubMed: 2345670]

Nagel S, Su Y, Horstmann S, Heiland S, Gardner H, Koziol J, Martinez-Torres FJ, Wagner S. Minocycline and hypothermia for reperfusion injury after focal cerebral ischemia in the rat: effects on BBB breakdown and MMP expression in the acute and subacute phase. Brain Res. 2008; 1188:198–206. [PubMed: 18031717]

Paolicelli RC, Bolasco G, Pagani F, Maggi L, Scianni M, Panzanelli P, Giustetto M, Ferreira TA, Guiducci E, Dumas L, Ragozzino D, Gross CT. Synaptic pruning by microglia is necessary for normal brain development. Science. 2011; 333:1456–8. [PubMed: 21778362]

Parakalan R, Jiang B, Nimmi B, Janani M, Jayapal M, Lu J, Tay SS, Ling EA, Dheen ST. Transcriptome analysis of amoeboid and ramified microglia isolated from the corpus callosum of rat brain. BMC Neurosci. 2012; 13:64. [PubMed: 22697290]

Rezaie P. Microglia in the Human Nervous System. Neuroembryology and Aging. 2003; 2:14.

Sheldon RA, Sedik C, Ferriero DM. Strain-related brain injury in neonatal mice subjected to hypoxia-ischemia. Brain Res. 1998; 810:114–22. [PubMed: 9813271]

Shrivastava K, Llovera G, Recasens M, Chertoff M, Gimenez-Llort L, Gonzalez B, Acarin L. Temporal expression of cytokines and signal transducer and activator of transcription factor 3 activation after neonatal hypoxia/ischemia in mice. Dev. Neurosci. 2013; 35:212–25. [PubMed: 23571161]

Soehnlein O, Lindbom L. Phagocyte partnership during the onset and resolution of inflammation. Nat. Rev. Immunol. 2010; 10:427–39. [PubMed: 20498669]

Stevens SL, Bao J, Hollis J, Lessov NS, Clark WM, Stenzel-Poore MP. The use of flow cytometry to evaluate temporal changes in inflammatory cells following focal cerebral ischemia in mice. Brain Res. 2002; 932:110–9. [PubMed: 11911867]

Uluc K, Kendigelen P, Fidan E, Zhang L, Chanana V, Kintner D, Akture E, Song C, Ye K, Sun D, Ferrazzano P, Cengiz P. TrkB receptor agonist 7, 8 dihydroxyflavone triggers profound gender-

dependent neuroprotection in mice after perinatal hypoxia and ischemia. CNS Neurol. Disord. Drug Targets. 2013; 12:360–70. [PubMed: 23469848]

Varin A, Gordon S. Alternative activation of macrophages: immune function and cellular biology. Immunobiology. 2009; 214:630–41. [PubMed: 19264378]

Verney C, Monier A, Fallet-Bianco C, Gressens P. Early microglial colonization of the human forebrain and possible involvement in periventricular white-matter injury of preterm infants. J. Anat. 2010; 217:436–48. [PubMed: 20557401]

Vexler ZS, Yenari MA. Does inflammation after stroke affect the developing brain differently than adult brain? Dev. Neurosci. 2009; 31:378–93.

Walton NM, Sutter BM, Laywell ED, Levkoff LH, Kearns SM, Marshall GP 2nd, Scheffler B, Steindler DA. Microglia instruct subventricular zone neurogenesis. Glia. 2006; 54:815–25. [PubMed: 16977605]

Wang J, Wei Q, Wang CY, Hill WD, Hess DC, Dong Z. Minocycline up-regulates Bcl-2 and protects against cell death in mitochondria. J. Biol. Chem. 2004; 279:19948–54. [PubMed: 15004018]

Wu X, Lu Y, Dong Y, Zhang G, Zhang Y, Xu Z, Culley DJ, Crosby G, Marcantonio ER, Tanzi RE, Xie Z. The inhalation anesthetic isoflurane increases levels of proinflammatory TNF-alpha, IL-6, and IL-1beta. Neurobiol. Aging. 2012; 33:1364–78. [PubMed: 21190757]

Xie Z, Culley DJ, Dong Y, Zhang G, Zhang B, Moir RD, Frosch MP, Crosby G, Tanzi RE. The common inhalation anesthetic isoflurane induces caspase activation and increases amyloid beta-protein level in vivo. Ann. Neurol. 2008; 64:618–27. [PubMed: 19006075]

Zhang Y, Xu Z, Wang H, Dong Y, Shi HN, Culley DJ, Crosby G, Marcantonio ER, Tanzi RE, Xie Z. Anesthetics isoflurane and desflurane differently affect mitochondrial function, learning, and memory. Ann. Neurol. 2012; 71:687–98. [PubMed: 22368036]

Highlights

- Hypoxia-ischemia induces an early microglial response in the hippocampus and a delayed response in the cortex and striatum.

- Minocycline treatment effectively suppressed microglial responses to HI in P9 and P30 mice.

- P9 minocycline-treated mice demonstrated an early but transient improvement in HI-induced neurologic injury.

- P30 minocycline-treated mice demonstrated sustained improvements in cerebral atrophy and memory at 60 days post-HI.

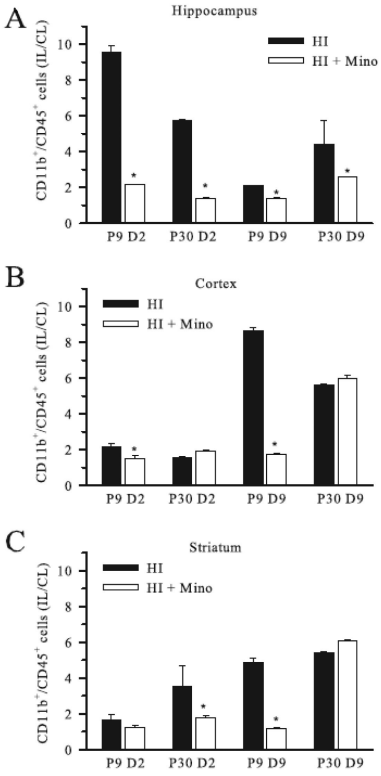

Figure 1. Effect of minocycline treatment on regional microglial counts post-HI

The number of $CD11b^+/CD45^+$ cells in ipsilateral hippocampus (**A**) cortex (**B**), and striatum (**C**) relative to the corresponding contralateral brain region (IL/CL) were determined using flow cytometry at either day 2 (D2) or day 9 (D9) post-HI in neonatal (P9) and juvenile (P30) mice treated with minocycline or vehicle. Data are mean ± sem. * = $p < 0.05$ vs untreated. n = 3 samples.

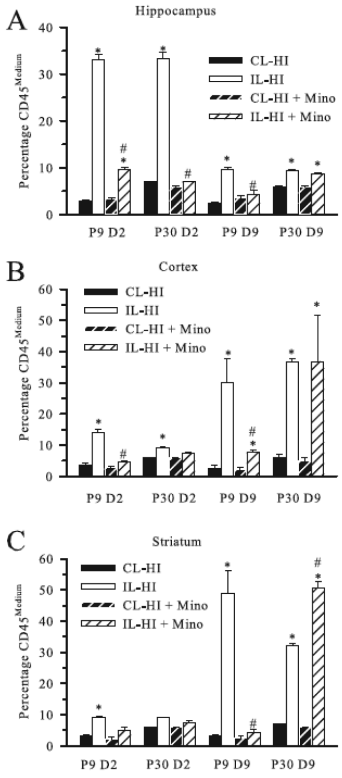

Figure 2. Effect of minocycline treatment on microglial activation post-HI

The percentage of $CD11b^{+}/CD45^{+}$ cell population demonstrating $CD45^{medium}$ expression (activated microglia) in contralateral (CL) and ipsilateral (IL) hippocampus (**A**) cortex (**B**), and striatum (**C**) at day 2 (D2) and day 9 (D9) post-HI are shown for P9 and P30 mice treated with minocycline or vehicle. Data are mean ± sem. * = $p < 0.05$ vs corresponding CL, # = $p < 0.05$ vs corresponding untreated IL. n = 3 samples.

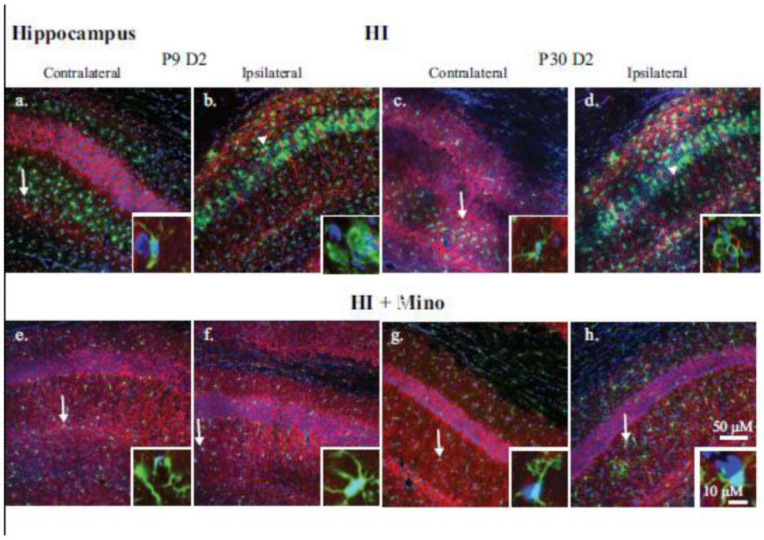

Figure 3. Immunohistological analysis of microglial response in the CA1 hippocampus

Double immunohistological staining for Iba1 (green) and MAP2 (red) proteins in the CA1 region of the hippocampus is shown. Nuclei were stained with DAPI (blue). **Upper panels**: the contralateral (**a, c**) and ipsilateral (**b, d**) hippocampi of P9 (**a, b**) and P30 (**c, d**) brains at 2 days post-HI are compared. **Lower panels**: the contralateral (**e, g**) and ipsilateral (**f, h**) hippocampi of P9 (**e, f**) and P30 (**g, h**) brains 2 days post-HI from minocycline-treated animals. **Insets**: magnification (240X) of representative microglia demonstrating either ramified (**arrow**) or amoeboid (**arrowhead**) morphology.

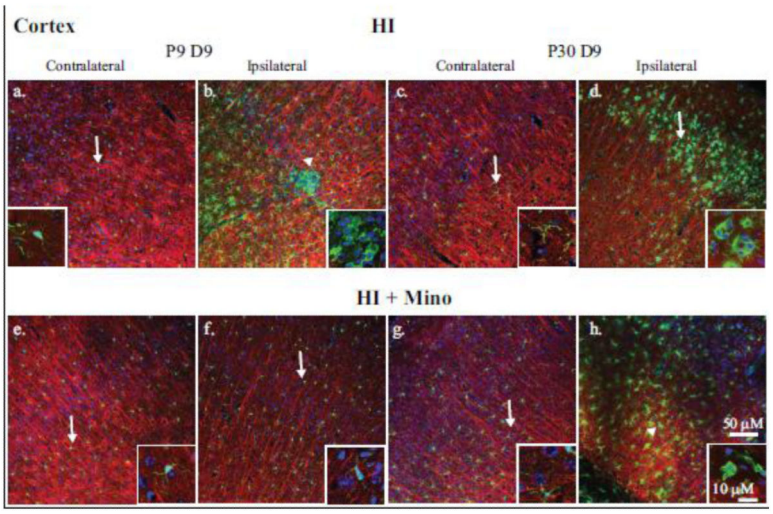

Figure 4. Immunohistological analysis of microglial response in the cortex

Double immunohistological staining for Iba1 (green) and MAP2 (red) proteins were examined in the cortex. Nuclei were stained with DAPI (blue). **Upper panels**: the contralateral (**a, c**) and ipsilateral (**b, d**) cortex of P9 (**a, b**) and P30 (**c, d**) brains at 9 days post-HI are compared. **Lower panels**: the contralateral (**e, g**) and ipsilateral (**f, h**) cortex of P9 (**e, f**) and P30 (**g, h**) brains at 9 days post-HI from minocycline-treated mice are compared. **Insets**: magnification (240X) of representative microglia demonstrating either ramified (**arrow**) or amoeboid (**arrowhead**) morphology.

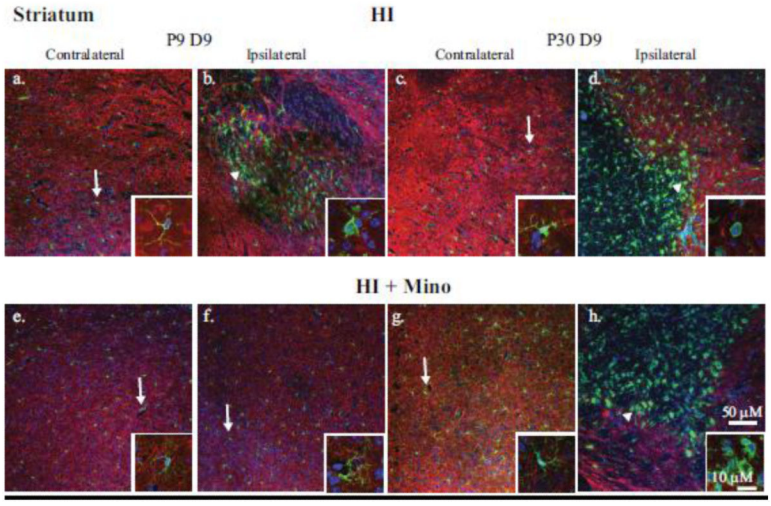

Figure 5. Immunohistological analysis of microglial response in the striatum

Double immunohistological staining for Iba1 (green) and MAP2 (red) proteins were examined in the striatum. Nuclei were stained with DAPI (blue). **Upper panels**: the contralateral (**a, c**) and ipsilateral (**b, d**) sides of P9 (**a, b**) and P30 (**c, d**) brains 9 days post-HI are compared. **Lower panels**: the contralateral (**e, g**) and ipsilateral (**f, h**) sides of P9 (**e, f**) and P30 (**g, h**) brains 9 days post-HI with minocycline treatment are compared. **Insets**: magnification (240X) of representative microglia demonstrating either ramified (**arrow**) or amoeboid (**arrowhead**) morphology.

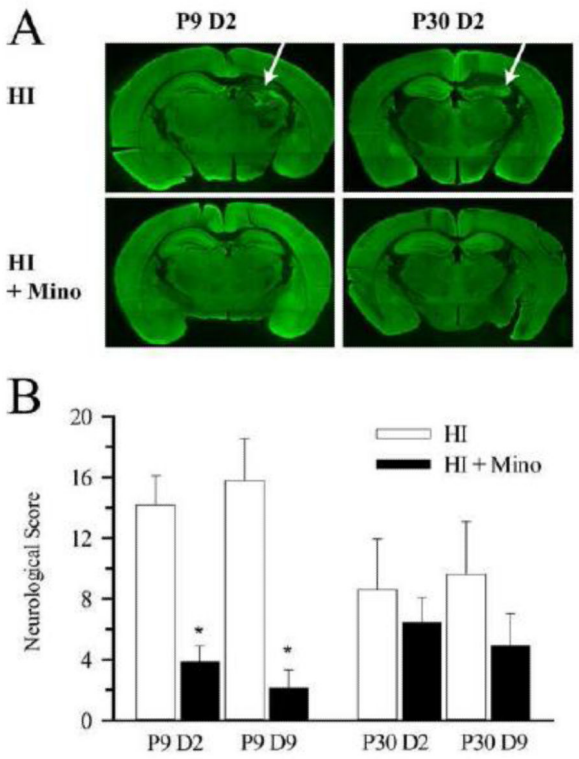

Figure 6. Effect of minocycline treatment on neurological damage at day 2 and day 9 post-HI.
A. Representative whole brain slices from P9 and P30 brains at day 2 post-HI with and without minocycline treatment are shown. **Arrow**: loss of hippocampal volume and MAP2 staining in the non-treated mice. **B.** Summary of neurological damage scores in P9 and P30 brains at day 2 (D2) and day 9 (D9) post-HI with and without minocycline treatment. * = $p < 0.05$ vs corresponding untreated. n = 8-14.

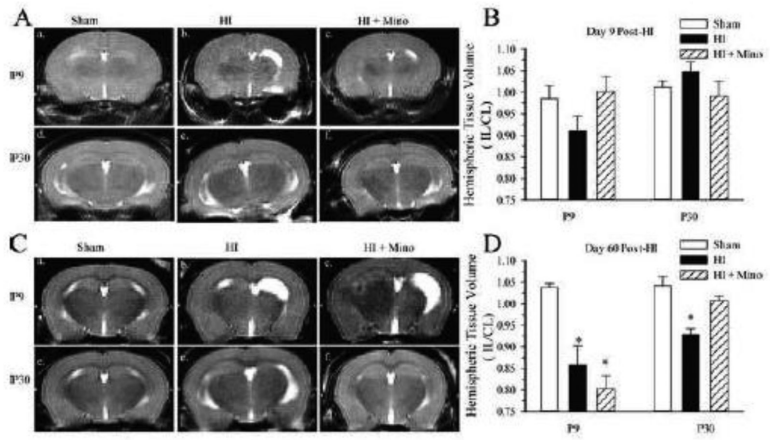

Figure 7. Effect of minocycline treatment on hemispheric volume post-HI

T2-weighted images were collected in P9 and P30 mice at day 9 and day 60 post-HI. **A**. Representative T2-weighted images from P9 Sham (**a**.), P9 HI (**b**.), P9 HI + minocycline-treated (**c**.), and P30 Sham (**d**.), P30 HI (**e**.), P30 HI + minocycline-treated (**f**.) at 9 days post-HI. **B**. Summary figure of T2-weighted ipsilateral hemispheric volumes normalized to the contralateral hemisphere (IL/CL) from P9 and P30 mice with and without minocycline treatment at day 9 post-HI. **C**. Representative T2-weighted images from P9 Sham (**a**.), P9 HI (**b**.), P9 HI + minocycline-treated (**c**.) and P30 Sham (**d**.), P30 HI (**e**.), P30 HI + minocycline-treated (**f**.) at 60 days post-HI. **D.** Summary figure of T2-weighted IL/CL hemispheric volumes from P9 and P30 mice with and without minocycline treatment at day 60 post-HI. Data are mean ± sem. * $p<0.05$ vs. sham, n = 5-8 treated and controls, 4-9 shams.

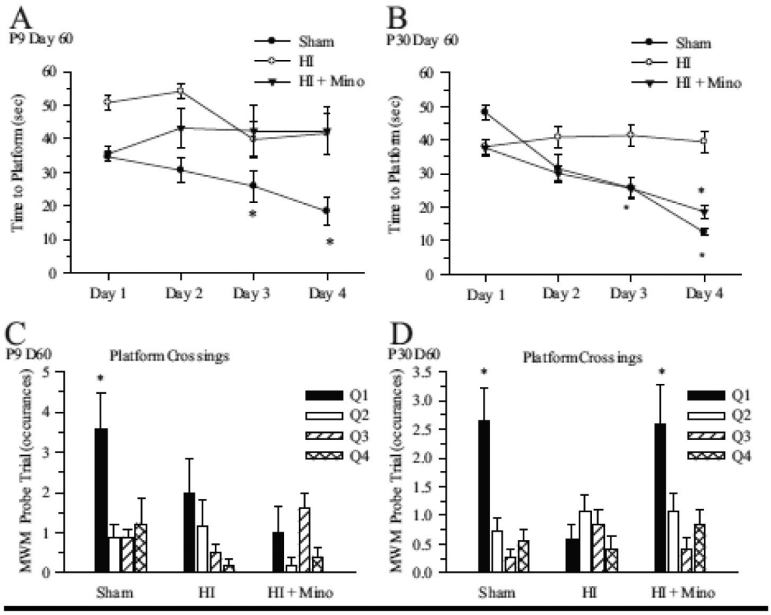

Figure 8. Effect of minocycline treatment on memory and learning at day 60 post-HI

Mice were subjected to HI at P9 or P30 with and without minocycline treatment and Morris water maze MWM testing was performed at 60 days post-HI. **A**. Summary figure of time to platform over the four days of training in sham, HI and HI + minocycline-treated P9 mice. Data are mean ± sem. n = 5-9 * $p < 0.05$ vs Day 1 value. **B**. Summary figure of time to platform over the four days of training in sham, HI and HI + minocycline-treated P30 mice. Data are mean ± sem. n = 11-12. * $p < 0.05$ vs Day 1 value. **C**. Summary of platform crossings for each quadrant in P9 sham, HI and HI + minocycline-treated mice. Q1 = Training Quadrant; *$p<0.05$, n=5-9. **D**. Summary of platform crossings for each quadrant in P30 sham, HI and HI + minocycline-treated mice. Q1 = Training Quadrant; *$p<0.05$, n=11-12.